Relativistic fluorescence yields for hollow atoms in the range $12 \leqslant Z \leqslant 56$

L. Natarajan
Department of Physics, University of Mumbai, Mumbai 400 098, India
(Received 28 August 2008; published 10 November 2008)

Energies and electric dipole rates of x rays from doubly ionized K shells of atoms in the range $Z=12$ to 56 have been calculated in the active space approximation using multiconfiguration Dirac-Fock wave functions with the inclusion of higher order relativistic corrections. Using a scaling procedure on the already available relativistic radial matrix elements for a single vacancy in the K shell, the Auger rates have been calculated for the empty K shell. The present investigation shows that though the contribution from relativistic correlation to the $K\alpha$ x-ray hypersatellite energies is not significant, the strength of correlation on the x-ray rates is appreciable, especially for low Z elements. It is observed that the contribution to single configuration $K\alpha_2^h$ rate of low Z ions is essentially from electron-electron correlation whereas Breit interaction contributes significantly to the $K\alpha_2^h$ rate of high Z elements. The $K\alpha_1^h$ rate is affected both by correlation and higher order relativistic corrections. The computed results for the x-ray and Auger transitions as well the fluorescence yields of double hole K shell of various ions are reported and compared with other available values.

DOI: 10.1103/PhysRevA.78.052505 PACS number(s): 32.30.−r, 31.15.−p

I. INTRODUCTION

The excitation and deexcitation of a hollow atom where the inner shell is completely empty have been studied by many researchers since it was first produced by Briand *et al.* in 1990 [1]. The structure properties of such atoms have wide ranging applications [2,3]. Moreover, as the inner shell is initially empty and hence relativistic, its decay properties give valuable information about the relativistic atomic correlation effects.

The radiative decay of empty inner shell has been experimentally investigated using different processes [1,4–7]. On the theoretical side, relativistic calculations using Dirac-Hartree-Slater (DHS) [8] and multiconfiguration Dirac-Fock (MCDF) [9–13] models are also available. The effects of Breit interaction and quantum electrodynamic corrections on the energies of $K\alpha$ X-ray hypersatellites have been studied in detail [8,9,11]. Although the radiative decay of double hole K shell has been studied extensively, information on the energies and rates of KK-KLL Auger transitions exist only for a few elements [12–16]. Neon appears to be the only element for which experimental observations on the energies and rates of Auger electrons from empty K shell are available [14–16]. Theoretical calculations using MCDF wave functions and including Breit and quantum electrodynamics corrections have been reported by Chen [13] on the x-ray and Auger decay of an empty K shell of five elements in the range $Z=10-36$. To the best of our knowledge, the only detailed information available on the fluorescence yields of a double hole K state of elements is that of Chen [13]. The purpose of the present investigation is to explore the contribution of electron-electron correlation to the $K\alpha$ x-ray hypersatellite rates and also to report on an extensive calculation of fluorescence yields of double hole K state of ions in the range $Z=12-56$.

In the present work, the energies and dipole rates of $K\alpha$ x-ray hypersatellites for sixteen elements have been computed in the relativistic configuration interaction formalism (RCI) which uses MCDF wave functions and includes Breit interaction, nuclear mass corrections, and quantum electrodyamic effects (QED) that are comprised mainly of self-energy and vacuum polarization. To account for correlation, single and double excitations of electrons in the active space approximation have been carried out. The Auger rates have been calculated by applying scaling factors to the already available relativistic Dirac-Hartree Slater (DHS) Auger radial matrix element [17] for the normal atomic configuration with a single vacancy in the K shell. The GRASPVU package used in the present work to generate the MCDF wave functions and perform the structure calculations is the modified version of the GRASP92 code [18,19].

II. NUMERICAL PROCEDURE

The relativistic MCDF basis set in the configuration interaction computational program is described in detail in the literature [18–20]. In the MCDF method, configuration state functions ϕ (ΓJ^P) of a certain J and parity are formed by taking a linear combination of Slater determinants of the Dirac orbitals. A linear combination of these configuration state functions (CSFs) is then used in the construction of atomic state functions (ASFs) with the same J and parity:

$$\Psi_i(J^P) = \sum_{\alpha=i}^{n_{\mathrm{CSF}}} C_{i\alpha}\phi(\Gamma_\alpha J^P), \tag{1}$$

where $C_{i\alpha}$ are the mixing coefficients for the state i and n_{CSF} are the number of CSFs included in the evaluation of ASF. The Γ_α represents all the one-electron and intermediate quantum numbers needed to define the CSFs. The ASFs thus constructed were used in solving the Dirac-Fock equation and the Dirac-Coulomb Hamiltonian included the Fermi charge distribution of the atomic nucleus. To improve the theoretical accuracy on the transition energies, the QED corrections which are essentially single-electron properties were taken from the recent rigorous compilations of Atremey *et al.* [21] by interpolation. As the code considers only the long wavelength limit of the two-photon transverse interaction, to

TABLE I. A comparison of relativistic configuration interaction energies in eV of $K\alpha_2^h$ and $K\alpha_1^h$ lines with other experimental and MCDF energy values.

	$K\alpha_2^h$			$K\alpha_1^h$		
		others			others	
Z	present	theory	expt.	present	theory	expt.
12	1367.7	1368.53[a]	1367.8 ± 0.2[d]	1373.6	1374.34[a]	
		1368.6[b]			1374.5[b]	
14	1874.5			1881.6		
18	3131.2	3131.5[a]		3141.4	3141.62[a]	
		3131.5[b]			3141.9[b]	
		3130.5[c]			3140.5[c]	
20	3884.8	3884.8[a]		3896.3	3896.39[a]	
22	4727.0	4723.86[a]	4727 ± 2[e]	4741.7	4736.76[a]	4741 ± 3[e]
		4723.7[b]			4737,6[b]	
24	5648.4	5646.5[b]	5650 ± 2[e]	5664.2	5663.4[b]	5666 ± 3[e]
			5645 ± 2[f]			
26	6657.0	6654.6[b]	6659 ± 2[e]	6675.9	6674.4[b]	6679 ± 3[e]
			6655 ± 2[f]			6675 ± 2[f]
			6658.3 ± 0.1[g]			6677.3 ± 0.8[g]
30	8928.9	8928.53[a]		8955.4	8954.97[a]	
		8926.8[c]			8953.2[b]	
36	12980.2	12978.3[a]		13031.5.	13029.3[a]	
		12979.7[b]			13035.8[b]	
		12975.1[c]			13028.7[c]	
38	14509.7			14577.2		
42	17837.1			17943.4		
46	21538.4			21697.2		
50	25619.7			25849.6		
54	30089.4	30086.1[b]		30414.9	30418.8[b]	
56	32480.5	32474.0[b]		32866.1	32865.6[b]	

[a]Reference [10].
[b]Reference [9].
[c]Reference [13].
[d]Reference [24].
[e]Reference [25].
[f]Reference [26].
[g]Reference [27].

obtain better predictions we added the frequency-dependent contributions of Cheng *et al.* [22] to our computed Breit energies. However, in the evaluation of transition rates, we considered only the frequency-independent part of Breit interaction in the Hamiltonian and recalculated the mixing coefficients while keeping the radial functions frozen. The nonorthogonality was taken into account in the evaluation of transition rates.

The Auger matrix elements between two CSFs can be separated into angular parts multiplied by radial integrals by using Racah algebra. Assuming a frozen orbital approximation, the values of DHS Auger electron radial matrix elements of atoms with a single initial vacancy were reported by Chen *et al.* [17]. The theoretical formalism for Auger electron emission probability in terms of first order perturbation theory is explained elsewhere [23].

The numerical procedure adopted in this work is mainly the same as in our earlier convergence study [12]. As a starting point, the CSFs were generated in the extended optimal level (EOL) scheme for the initial configuration with empty $1s$ shell and final configuration with a vacancy in the $1s$ and $2p$ shells. In the EOL method, the radial orbitals and the mixing coefficients are determined by optimizing the energy functional which is the weighted sum of the energy values corresponding to a set of $(2j+1)$ eigenstates. The zero order eigenfunctions and energy eigenvalues were first calculated using this code. The generation of CSFs depends on the correlation model and the orbital set in the active space. In this work, in the case of atoms with open shell ground state configuration, the coupling between the inner shell vacancies and the outer incomplete subshells was not taken into account. However, the electron-electron correlation was in-

TABLE II. $K\alpha_2^h$ and $K\alpha_1^h$ x-ray rates in 10^{14} s^{-1} in length gauge calculated with the inclusion of correlation, Breit interaction and quantum electrodynamic corrections. Also listed are the earlier MCDF length gauge [13] and DHS total rates [8]. The asterisk indicates the previous DHS total rates.

	X-ray rates				
	$K\alpha_2^h$		$K\alpha_1^h$		
Z	present	Ref. [13]	present	Ref. [13]	Ref. [8]
12	0.547		0.00041		
14	1.032		0.0171		
18	2.929	3.07	0.0399	0.043	2.718*
20	4.487		0.129		4.279*
22	5.609		0.489		
24	8.624		1.286		
26	10.52		2.281		
30	17.93	18.3	7.047	7.205	23.88-
36	29.56	29.7	22.47	23.9	50.93*
38	33.79		31.82		
42	46.12		52.55		
46	61.41		81.28		
48	70.09		98.81		
50	81.82		118.32		
54	107.8		165.29		
56	123.2		83.01		269.6*

cluded by considering the excitations of atomic orbitals in the active space approximation. The RCI requirements are different for different initial ground state configurations. For atoms with unfilled outer shells, the correlation functions were evaluated by considering an active set with $1s$, $2p$, and unfilled orbitals and the other virtual orbitals that are in the same major shell as the unfilled subshell. For some elements, the virtual shells in the subsequent major shell were also included. For example, the relativistic ground state configuration of Si is $[\mathrm{Ne}]3s^2 3p_{1/2}^2$ and the active set was taken to be $[1s_{1/2}, 2p_{1/2}, 2p_{3/2}, 3p_{1/2}, 3p_{3/2}, 4s_{1/2}, 4p_{1/2}, 4p_{3/2}]$. For closed shell configurations, the active set consisted of reference configurations and a few unfilled shells outside the closed shell configuration. In the case of Ar, the expansion set consisted of $\{1s_{1/2}, 2p_{1/2}, 2p_{3/2}, 4s_{1/2}, 3d_{3/2}, 3d_{5/2}, 4p_{1/2}, 4p_{3/2}\}$ orbitals. Inclusion of any additional orbitals did not contribute to the mixing coefficients. The correlation was evaluated by considering single and double excitations of electrons from the reference configurations to the orbitals in the active set taking into account convergence criteria which in this work was taken to be 10^{-8}. In the present work, the initial state configurations of Cr and Mo were taken to be $[\mathrm{Ar}]4s^2 3d_{3/2}^4$ and $[\mathrm{Kr}]5s^2 4d_{3/2}^4$, respectively, and it was assumed that the contributions from the respective $3d_{5/2}$ and $4d_{5/2}$ electron will not alter the transition energies and rates significantly.

The Auger rates were calculated by applying scaling factors to the relativistic Auger matrix elements. The Auger radial matrix elements for singly ionized atoms have been reported by Chen *et al.* [17] using *jj* coupled Dirac-Hartree-Slater (DHS) wave functions. In our earlier work [12], these values were used to calculate the radial matrix elements of neon with an empty K shell and varying degrees of ionization in the L shell. In a similar way, in this work the radial integral values of Chen *et al.* were modified by including scaling parameters to the radial integral values of K-L_1L_1, K-L_1L_{23}, and K-$L_{23}L_{23}$ transitions In this work, these correction factors were taken as the ratios of the correlated electron densities for the atom with triple hole KL_1L_1, KL_1L_{23} and $KL_{23}L_{23}$ configurations and the respective double hole L_1L_1, L_1L_{23}, and $L_{23}L_{23}$ configurations at the position of the

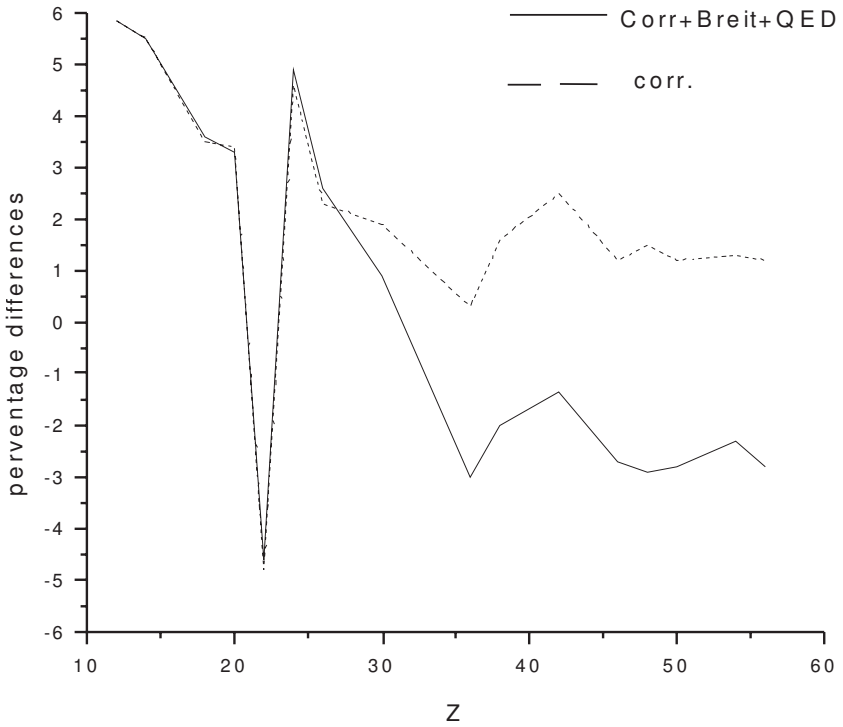

FIG. 1. Percentage differences between length gauge $K\alpha_2^h$ rates and single configuration rates. Solid line indicates Breit and quantum electrodynamic corrections along with electron-electron correlation while dashed line refers to contribution from correlation only.

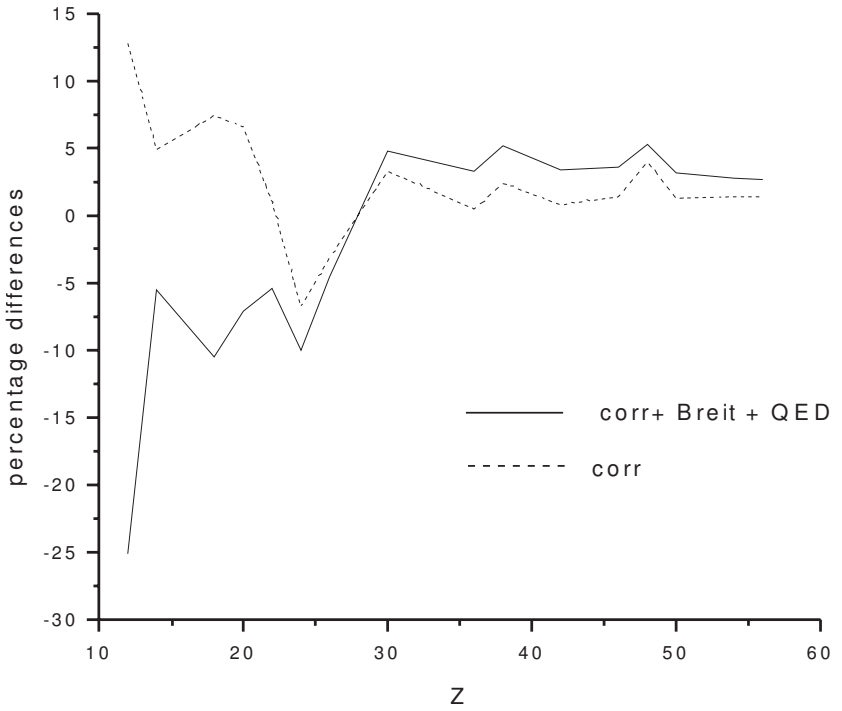

FIG. 2. Percentage differences between length gauge $K\alpha_1^h$ rates and single configuration rates. Solid line indicates calculations with contributions from Breit interaction, quantum electrodynamic corrections and electron-electron correlation while dashed line refers to contribution from correlation only.

nucleus. As the Auger rates are independent of the passive electron structure and initial double hole K state will affect substantially in altering the single K hole radial matrix elements, the present Auger rates are expected to be accurate. Also, it has been shown by Chen *et al.* [8] that the DHS results agree well with the results of MCDF calculations and the DHS model can be relied upon to get results of adequate accuracy.

III. RESULTS AND DISCUSSION

The contributions from correlation to the $K\alpha$ x-ray hypersatellite energies was observed to be unimportant by Martins *et al.* [10]. However, the effect of correlation on the transition rates of double hole K state has not been explored. To analyze this contribution of electron-electron correlation to the transition parameters, we first investigated the effect of correlation on the transition energies and rates. We then carried out another set of calculations that included correlation, Breit interaction, and quantum electrodynamic corrections. Our results also show that the effect of correlation on the transition energies is negligible and contributes, in general, between 3 to 6 eV for both the $K\alpha_2^h$ and $K\alpha_1^h$ lines of all the elements. The computed RCI energies that include both correlation and higher order relativistic corrections are com-

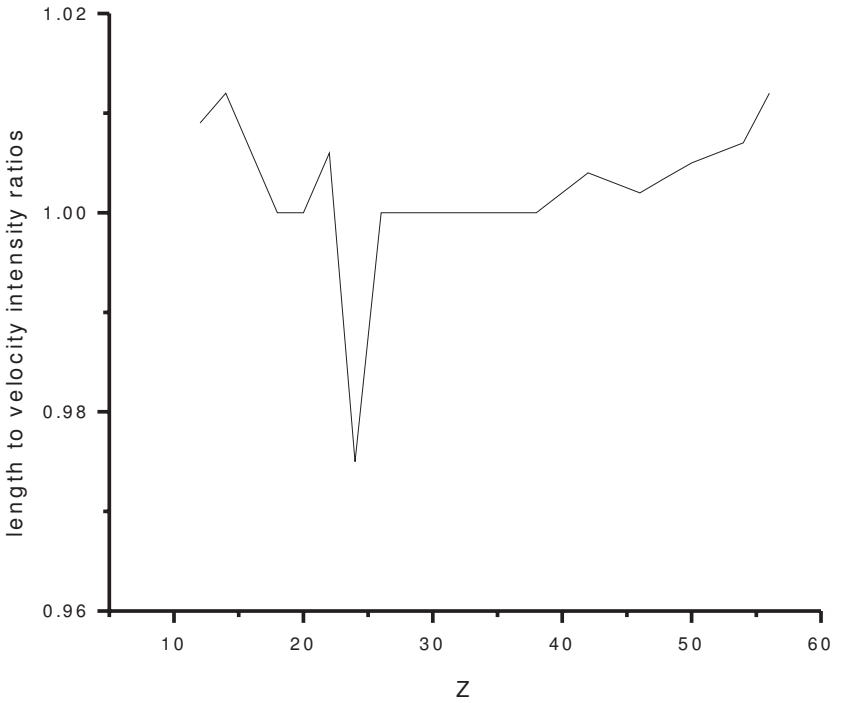

FIG. 3. Ratios of $\frac{I(K\alpha_1^h)}{I(K\alpha_2^h)}$ calculated in length to velocity gauge.

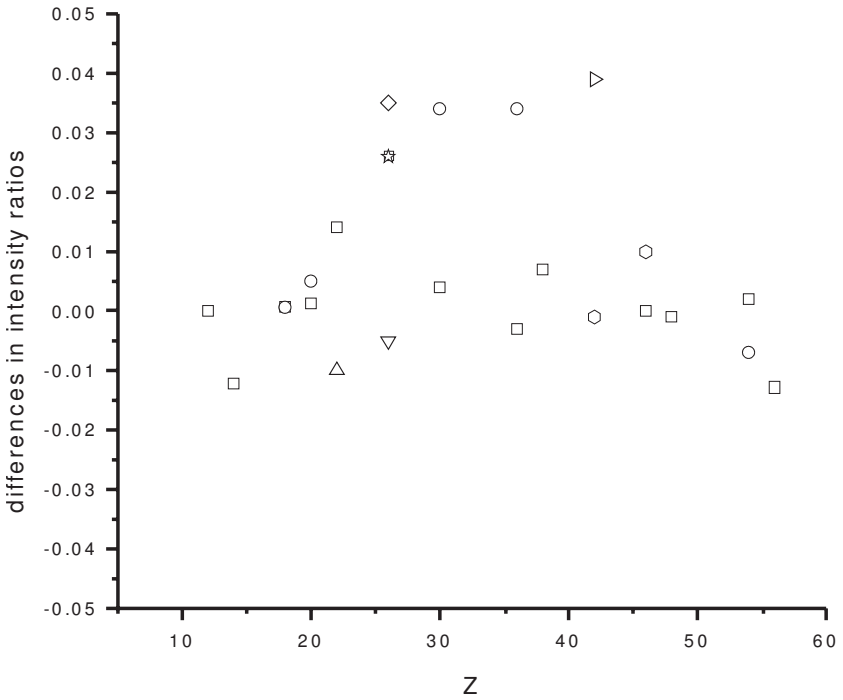

FIG. 4. Differences between the RCI intensity ratios calculated in this work and other theoretical and experimental ratios. Square, present; circle, Ref. [11]; triangle, Ref. [18]; inverted triangle, MCDF Ref. [27]; reverse square, experiment in Ref. [27]; left triangle, Ref. [26]; right triangle, Ref. [25]; hexagon, Ref. [29]; star, Ref. [28].

pared in Table I with other theoretical and experimental energies. Since the present study tries to analyze the contribution of correlation to the transition parameters and Breit as well other QED corrections are of interest here, only results from similar earlier investigations are listed. The agreement between the present $K\alpha_2^h$ line energies and earlier experimental measurements on Mg [24], Ti [25], Cr [25,26], and Fe [25–27] is very good within the experimental uncertainties. The RCI energies differ from the relativistic mono-configuration values of Martins *et al.* [10] by <0.5 eV except for $Z=22$ for which the difference is ~ 3 eV. The present calculations include higher order relativistic corrections and electron-electron correlation but neglects coupling between the initial as well the final vacancy states and the unfilled outer shells whereas the single configuration energies of Martins *et al.* [10] neglects correlation but considers full Breit interaction and QED corrections and also includes the coupling with the outer open shells. However, it is observed that both the approaches yield nearly the same transition energies. The RCI energies are in good agreement with the earlier MCDF results of Chen [13] except for $Z=36$ for which the RCI energies differ from MCDF values of Chen

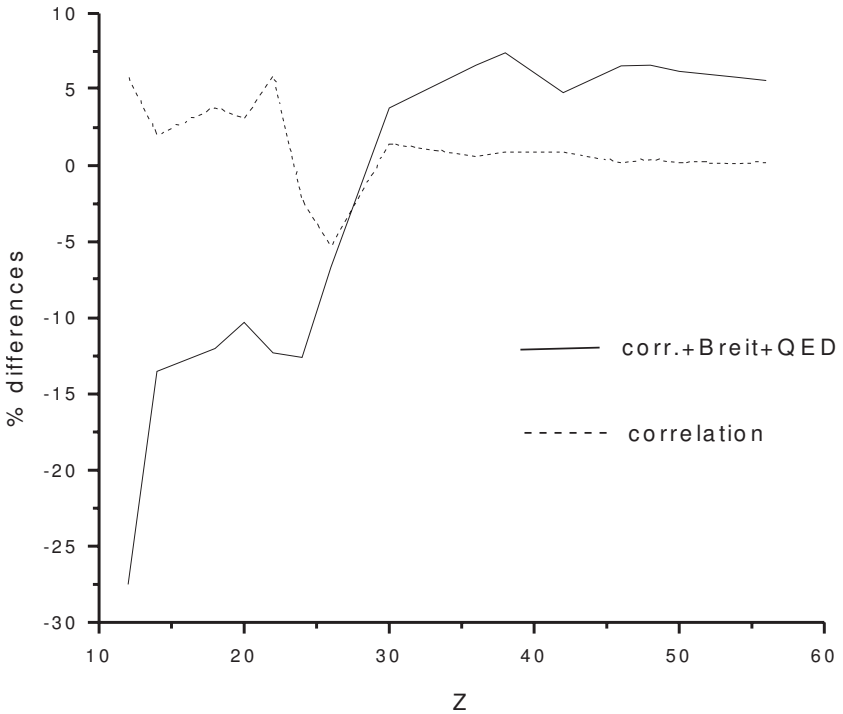

FIG. 5. Percentage differences between length gauge intensity ratios of $K\alpha_1^h$ to $K\alpha_1^h$ line and single configuration ratios. Solid line indicates calculations with contributions from Breit interaction, quantum electrodynamic corrections and electron-electron correlation while dashed line refers to contribution from correlation only.

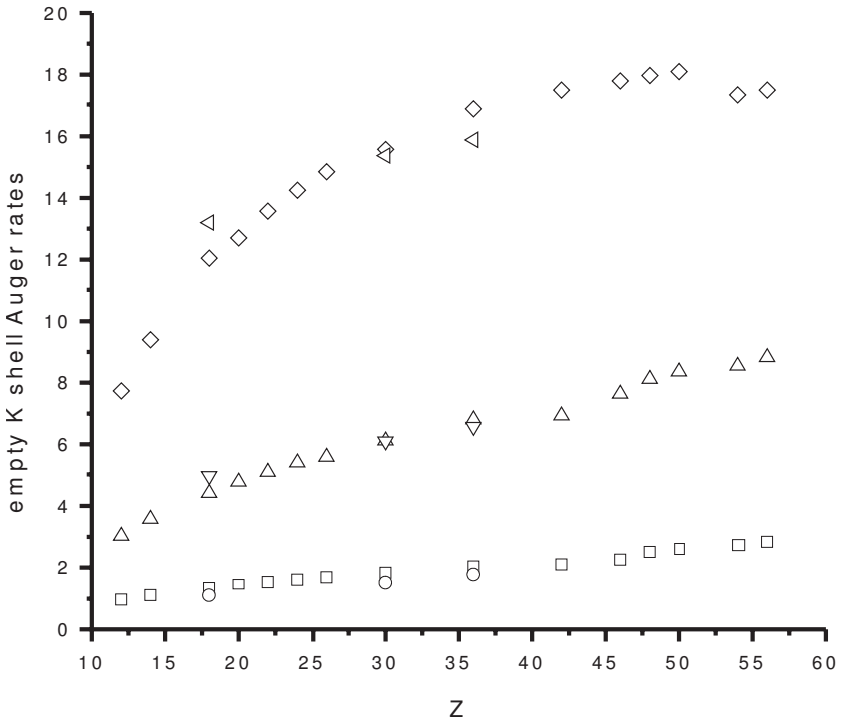

FIG. 6. Empty K shell Auger rates in 10^{14} s^{-1}. Squares, triangles and reverses square are the rates KK-KL_1L_1, KK-L_1L_{23} and KK-$KL_{23}L_{23}$ calculated in this work. Circles, inverted triangles, and left triangles are the respective MCDF rates of above three transitions reported by Chen [13].

by ~5 eV. The overall agreement between the present energies and the relativistic values of Aberg *et al.* [9] is good. The energies of $K\alpha_1^h$ lines are also in very good agreement with the experimental and earlier theoretical results.

In Table II, the RCI length gauge dipole rates of $K\alpha_2^h$ and $K\alpha_1^h$ lines of various elements are reported along with the length gauge MCDF rates of Chen [13] and the total DHS rates of Chen *et al.* [8]. The present rates are smaller than the MCDF rates of Chen for $Z=18$, 30, and 36 by ~4, 2, and 3 %, respectively, and this might be due to second order correction from correlation to the x-ray rates. The present total rates of $K\alpha^h$ lines are larger than the DHS rates of Chen *et al.* [8] by 1–4 % except for $Z=18$ and 20.

The percentage differences between the length gauge RCI and single configuration DF rates of $K\alpha_2^h$ lines with respect to DF rates for various Z are plotted in Fig. 1. To analyze the influence of correlation on the dipole rates, similar length gauge percentage differences between the correlated and DF rates of $K\alpha_2^h$ lines are also plotted in the same figure. While correlation coupled with higher order relativistic corrections enhance the DF rates for $Z \leqslant 30$ except for $Z=22$ and reduce the single configuration rates for $Z>30$, the contribution from only correlation enhances the DF rates for all Z except for $Z=22$. Our calculations show that though the influence of correlation on the energies of $K\alpha_2^h$ x ray is negligible, the effect of electron-electron correlation on the dipole rates vary with atomic number. It is observed that the RCI rates and correlated rates of $K\alpha_2^h$ line are nearly the same for $Z \leqslant 26$ showing that the contribution of correlation to the EI rate is significant and the overall effect of higher order relativistic corrections on the rate is only marginal, while for medium and heavy elements, the x-ray rates are sensitive to Breit interaction. The strength of correlation on the length and velocity rates varies with atomic number and the trend is irregular.

In Fig. 2, the percentage differences between the RCI and monoconfiguration rates of $K\alpha_1^h$ lines with respect to single-configuration rates calculated in length gauge are plotted for various Z. Similar percentage differences between the dipole rates of $K\alpha_1^h$ line investigated with and without correlation are also plotted in the same figure. Unlike $K\alpha_2^h$ rates, the RCI rates for $K\alpha_1^h$ lines are smaller than the DF rates for light atoms and larger for $Z \geqslant 30$. The variations between RCI and monoconfiguration rates range from 3–6 % for $Z \geqslant 30$. For the other low Z elements, the variations are more than 10% with a maximum of 25% for $Z=12$. The correlation enhances the $K\alpha_1^h$ rates of all except for $Z=24$ and 26 with a reduction of 6.8 and 3.1 %, respectively. It is observed that correlation in general affects the velocity rates of $K\alpha_1^h$ line slightly more than the length rates except for a few ions. It is also seen that though the contribution of Breit interaction to the dipole rate of $K\alpha_2^h$ line is negligible for low Z elements, its influence on the $K\alpha_1^h$ rate of these ions is significant.

As observed in our earlier work [30], this work also confirms that EOL calculations lead to correct nonrelativistic (NR) limit when the major contributions from $1s2p_{3/2}$ and $1s2p_{1/2}$ states are considered and the contributions from other correlation configurations retain to a larger extent the proportionality of the mixing coefficients of $^3P_1$ and $^1P_1$ states in the NR limit.

The ratios of $\frac{I(K\alpha_1^h)}{I(K\alpha_2^h)}$ calculated in length to velocity gauges are presented in Fig. 3. The length values are nearly the same as the velocity ratios for most of the elements with a maximum of 1.012 for $Z=14$ and 56 and a minimum of 0.975 for $Z=24$. The near equal agreement between the intensity ratios calculated in length and velocity gauges gives a measure of the accuracy of the wavefunctions employed in this work.

In Fig. 4, the differences between the present intensity ratios of $K\alpha_1^h$ to $K\alpha_2^h$ lines calculated in length gauge and earlier relativistic values [8,11] are plotted for various Z.

Also included are the differences between the present ratios and the experimental ratios of Ti [25], Fe [25–27], and the experimental as well the MCDF ratios of Mo [28,29] and Pd [29]. While the present ratios are in good agreement with the experimental value of Ti [25] and Mo [28], they underestimate the experimental values of Boscheng *et al.* [29] for Mo and Pd by ~16 and 27 %, respectively. However, the RCI values are in good agreement with their MCDF ratios. The RCI ratios are larger than the velocity gauge ratios of Costa *et al.* [11] for light elements except for $Z=14$ and the differences between the two results indicate the sensitivity of transition rates of low Z ions to correlation and for $Z \geqslant 30$, the present ratios are in excellent agreement with their values confirming that the contributions from Breit interaction and QED corrections to the $E1$ rates are significant while the effect of correlation is negligible for medium and high Z ions. The RCI ratios are larger than the DHS rates of Chen *et al.* [8] by 1 to 5 % with the exception of $Z=22$.

The percentage differences between RCI and monoconfiguration relative intensities of fine structure lines with respect to the single configuration rates are plotted in Fig. 5 for various Z. Similar percentage differences between the intensity ratios of these lines calculated with and without correlation are also included in the same figure. It is clear from the figure that correlation along with higher order relativistic corrections reduce the intensity ratios of low Z ions and enhance the ratios of ions with $Z \geqslant 30$, whereas contribution from only correlation in general enhances these ratios. With increasing Z, the contribution of correlation to intensity ratios is nearly a constant and is $<1\%$.

In Fig. 6, the calculated Auger rates for the KK-KL_1L_1, KK-L_1L_{23}, and KK-$Kl_{23}L_{23}$ transitions are plotted as a function of Z. Also included are the length gauge rates of Chen [13] for these transitions for $Z=18$, 30, and 36. The scaled DHS rates are slightly larger than the MCDF rates of Chen for KK-KL_1L_1 transition. However, the present rates are in good agreement with the MCDF rates of Chen for the KK-KL_1L_{23} and KK-$L_{23}L_{23}$ transitions and differ by 2–4 % This reasonably good agreement indicates that the scaled DHS matrix elements are as reliable as MCDF values in the evaluation of KK-KLL Auger hypersatellite rates.

Table III lists the fluorescence yields of the empty K shell and includes the MCDF fluorescence yields of Chen [13] for $Z=18$, 30, and 36. The present values are in good agreement with those of Chen and the marginal difference is due to the fact that the relativistic x-ray rates of Chen include the contributions from the $1s$-$3p$ transition also.

TABLE III. Double hole K shell fluorescence yields. Also listed are the MCDF yields of Chen [13].

	fluorescent yields	
Z	present	Ref. [13]
12	0.0446	
14	0.0695	
18	0.140	0.135
20	0.192	
22	0.232	
24	0.316	0.309
26	0.367	
30	0.515	0.505
36	0.663	0.659
42	0.770	
46	0.837	
48	0.855	
50	0.877	
54	0.880	
56	0.913	

IV. CONCLUSIONS

The transition energies and rates of x rays from the empty K shell of atoms in the range $Z=12$ to 56 have been reported. While the monoconfiguration rate of $K^h_{\alpha 2}$ x rays from low Z ions is altered mainly by electron-electron correlation, Breit interaction contributes significantly to high Z ions. The $K\alpha^h_1$ rate is affected both by correlation and higher order relativistic corrections. While correlation in general enhances the $K\alpha^h_1$ rate, Breit interaction reduces the rate of low Z atoms and enhances the rate of high Z elements. The empty K shell configuration average Auger rates calculated using relativistic DHS radial matrix elements of singly ionized K shell are found to be in good agreement with the MCDF rates thereby ensuring that the simple approach, used in this work is reliable in the evaluation of double hole K shell Auger rates with a reasonably good degree of accuracy.

ACKNOWLEDGMENTS

This work was supported by the project financed by the Department of Science and Technology, Government of India, New Delhi, India.

[1] J. P. Briand, L. de Billy, P. Charles, S. Essabaa, P. Briand, R. Getter, J. P. Desclaux, S. Billman, and C. Restori, Phys. Rev. Lett. **65**, 159,(1990).

[2] R. Diamant, S. Huotari, K. Hämäläinen, C. C. Kao, and M. Deutsch, Phys. Rev. Lett. **84**, 3278 (2000).

[3] K. Moribayashi, A. Sasaki, and T. Tajima, Phys. Rev. A **59**, 2732 (1999).

[4] R. L. Kauffman and P. Richard, in *Methods of Experimental Physics* edited by D. Williams (Academic, New York, 1976), p. 48.

[5] J. P. Briand, P. Chevallier, A. Johnson, J. P. Rozet, M. Tavernier and A. Touati, Phys. Lett. **49A**, 51 (1974).

[6] R. L. Watson, O. Benka, K. Parthasarathi, R. J. Maurer, and J. M. Sanders, J. Phys. B **16**, 835 (1983).

[7] O. Keski-Rahkonen, J. Saijonmaa, M. Suvanen, and A. Servomaa, Phys. Scr. **16**, 105 (1977).
[8] M. H. Chen, B. Crasemann, and H. Mark, Phys. Rev. A **25**, 391 (1982).
[9] T. Aberg, in *Advances in X-ray Spectroscopy*, edited by C. Bonnelle and C. Mande (Pergamon, New York, 1982) p. 1.
[10] M. C. Martins, A. M. Costa, J. P. Santos, F. Parente, and P. Indelicato, J. Phys. B **37**, 3785 (2004).
[11] A. M. Costa, M. C. Martins, J. P. Santos, P. Indelicato, and F. Parente, J. Phys. B **40**, 57 (2007).
[12] L. Natarajan, Phys. Scr. **75**, 47 (2007).
[13] M. H. Chen, Phys. Rev. A **44**, 239 (1991).
[14] Z. Smit, M. Zitnik, L. Avaldi, R. Camilloni, E. Fainelli, A. Muhleisen, and G. Stefani, Phys. Rev. A **49**, 1480 (1994).
[15] P. Pelicon, I. Cadez, M. Zitnik, Z. Smit, S. Dolenc, A. Muhleisen, and R. I. Hall, Phys. Rev. A **62**, 022704 (2000).
[16] S. H. Southworth, E. P. Kanter, B. Krassig, L. Young, G. B. Armen, J. C. Levin, D. L. Ederer, and M. H. Chen, Phys. Rev. A **67**, 062712 (2003).
[17] M. H. Chen, F. P. Larkins, and B. Crasemann, At. Data Nucl. Data Tables **45**, 1 (1990).
[18] P. Jonsson, X. He, and C. Froese Fischer, The GRASPVU relativistic atomicstructure package, Technical Report DOE/ER/US Department of Energy, 1998.
[19] F. A. Parpia, C. Froese Fischer, and I. P. Grant, Comput. Phys. Commun. **94**, 249 (1996).
[20] K. G. Dyall, I. P. Grant, C. T. Johnson, F. A. Parpia, and E. P. Plummer, Comput. Phys. Commun. **55**, 425 (1989).
[21] A. N. Artemyev, V. M. Shabaev, V. A. Yerokhin, G. Plunien, and G. Soff, Phys. Rev. A **71**, 062104 (2005).
[22] K. T. Cheng, M. H. Chen, W. R. Johnson, J. Sapirstein, Phys. Rev. A **50**, 247 (1994).
[23] M. H. Chen, E. Laiman, B. Crasemann, M. Aoyagi, and H. Mark, Phys. Rev. A **19**, 2253 (1979).
[24] E. Mikkola, O. Keski-Rahkonen, and R. Kuoppala, Phys. Scr. **19**, 29 (1979).
[25] J. Ahopelto, E. Rantavouri, and O. Keski-Rahkonen, Phys. Scr. **20**, 71 (1979).
[26] S. I. Salem, A. Kumar, and B. L. Scott, Phys. Rev. A **29**, 2634 (1984).
[27] R. Diamant, S. Huotari, K. Hämäläinen, C. C. Kao, and M. Deutsch, Phys. Rev. Lett. **84**, 3278 (2000).
[28] S. I. Salem, Phys. Rev. A **21**, 858 (1980).
[29] B. Boschung, J.-Cl. Dousse, B. Galley, Ch. Herren, J. Hoszowska, J. Kern, Ch. Rheme, Z. Halabuka, T. Ludziejewski, P. Rymuza, Z. Sujkowski, and M. Polasik, Phys. Rev. A **51**, 3650 (1995).
[30] L. Natarajan and Anuradha Natarajan, Phys. Rev. A **75**, 062502 (2007).